Published OnlineFirst March 20, 2019; DOI: 10.1158/0008-5472.CAN-18-1220

Cancer Research

4E-BP1 Is a Tumor Suppressor Protein Reactivated by mTOR Inhibition in Head and Neck Cancer

Zhiyong Wang[1,2], Xiaodong Feng[1], Alfredo A. Molinolo[1], Daniel Martin[3], Lynn Vitale-Cross[3], Nijiro Nohata[1], Mizuo Ando[1], Amy Wahba[4], Panomwat Amornphimoltham[1,5], Xingyu Wu[1], Mara Gilardi[1], Michael Allevato[1,6], Victoria Wu[1,6], Dana J. Steffen[1,6], Philip Tofilon[4], Nahum Sonenberg[7], Joseph Califano[1], Qianming Chen[2], Scott M. Lippman[1], and J. Silvio Gutkind[1,6]

Abstract

Aberrant activation of the PI3K–mTOR signaling pathway occurs in >80% of head and neck squamous cell carcinomas (HNSCC), and overreliance on this signaling circuit may in turn represent a cancer-specific vulnerability that can be exploited therapeutically. mTOR inhibitors (mTORi) promote tumor regression in genetically defined and chemically induced HNSCC animal models, and encouraging results have been recently reported. However, the mTOR-regulated targets contributing to the clinical response have not yet been identified. Here, we focused on *EIF4E-BP1* (*4E-BP1*), a direct target of mTOR that serves as key effector for protein synthesis. A systematic analysis of genomic alterations in the *PIK3CA*–mTOR pathway in HNSCC revealed that *4E-BP1* is rarely mutated, but at least one *4E-BP1* gene copy is lost in over 35% of the patients with HNSCC, correlating with decreased 4E-BP1 protein expression. *4E-BP1* gene copy number loss correlated with poor disease-free and overall survival. Aligned with a tumor-suppressive role, *4e-bp1/2* knockout mice formed larger and more lesions in models of HNSCC carcinogenesis. mTORi treatment or conditional expression of a mutant 4E-BP1 that cannot be phosphorylated by mTOR was sufficient to disrupt the translation–initiation complex and prevent tumor growth. Furthermore, CRISPR/Cas9–targeted *4E-BP1* HNSCC cells resulted in reduced sensitivity to mTORi *in vitro* and *in vivo*. Overall, these findings indicate that in HNSCC, mTOR persistently restrains 4E-BP1 via phosphorylation and that mTORi can restore the tumor-suppressive function of 4E-BP1. Our findings also support 4E-BP1 expression and phosphorylation status as a mechanistic biomarker of mTORi sensitivity in patients with HNSCC.

Significance: These findings suggest that EIF4E-BP1 acts as a tumor suppressor in HNSCC and that 4E-BP1 dephosphorylation mediates the therapeutic response to mTORi, providing a mechanistic biomarker for future precision oncology trials.

Introduction

Each year, approximately 600,000 new cases of head and neck squamous cell carcinoma (HNSCC), including cancers the oral cavity, oropharynx, larynx, and hypopharynx, are diagnosed worldwide, resulting in 300,000 deaths, 13,000 of which occur in the United States alone (1). The main risk factors for HNSCC include tobacco and alcohol use and high-risk human papillomavirus (HPV) infection (2). The incidence of HNSCC is rising with the increasing incidence of HPV^+ oropharyngeal cancer (3). HNSCC has a poor 5-year survival rate, approximately 63% (1), which emphasizes the urgent need to develop new effective options to prevent and treat this malignancy.

Early studies by our team revealed that aberrant activation of the PI3K–mTOR signaling network is one of the most frequent molecular alterations in HNSCC (4–6). Indeed, this study of a large collection of HNSCC tissues and multiple HNSCC mouse models have provided evidence that PI3K–mTOR activation is an early and necessary step for HNSCC development. The underlying molecular mechanisms resulting in pathway over activity have been recently elucidated by next-generation sequencing approaches as part of The Cancer Genome Atlas (TCGA) network (7–10). This large deep-sequencing initiative has revealed numerous mutations, copy number variations, and altered DNA methylation profiles in individual HNSCC lesions, thus providing an in-depth genomic characterization of HNSCC (7–10). Of interest, the PI3K–mTOR circuitry is among the most commonly altered signaling mechanisms. In particular, multiple genetic and epigenetic changes, including frequent *PIK3CA* mutations and gene copy number gain, and *PTEN* gene copy number loss and

[1]Moores Cancer Center, University of California, San Diego, La Jolla, California. [2]State Key Laboratory of Oral Diseases, National Clinical Research Center for Oral Diseases, West China Hospital of Stomatology, Sichuan University, Chengdu, China. [3]National Institute of Dental and Craniofacial Research, National Institutes of Health, Bethesda, Maryland. [4]National Cancer Institute, National Institutes of Health, Bethesda, Maryland. [5]International College of Dentistry, Walailak University, Nakhon Si Thammarat, Thailand. [6]Department of Pharmacology, University of California, San Diego, La Jolla, California. [7]Department of Biochemistry and Goodman Cancer Centre, McGill University, Montreal, Quebec, Canada.

Note: Supplementary data for this article are available at Cancer Research Online (http://cancerres.aacrjournals.org/).

Corresponding Authors: J. Silvio Gutkind, University of California, San Diego, 3855 Health Sciences Drive, La Jolla, CA 92093. Phone: 858-534-5980; E-mail: sgutkind@ucsd.edu; Scott M. Lippman, slippman@ucsd.edu; and Qianming Chen, West China Hospital of Stomatology, Sichuan University, Chengdu, Sichuan 610041, China. E-mail: qmchen@scu.edu.cn

doi: 10.1158/0008-5472.CAN-18-1220

Published OnlineFirst March 20, 2019; DOI: 10.1158/0008-5472.CAN-18-1220

mutations, converge to sustain persistent aberrant PI3K–mTOR pathway activation in HNSCC (reviewed in refs. 10 and 11). In turn, the overreliance on this pathway for HNSCC progression and metastasis may represent a vulnerability that can be exploited therapeutically for HNSCC treatment.

In this regard, mTOR inhibition is quite effective in promoting the regression of tumor lesions in multiple HNSCC xenografts, as well as in chemically induced and genetically defined HNSCC mouse models (4, 6, 12, 13). These findings provided the rationale for launching a phase IIb clinical trial targeting mTOR with its allosteric inhibitor, rapamycin, in patients with HNSCC in the neoadjuvant setting (14). This trial (NCT01195922), which was recently completed, achieved objective clinical responses (≥30% tumor volume reduction, including a complete pathologic response) in 25% of the patients, in spite of a short duration of the trial (3 weeks; ref. 14). However, given the extraordinary complexity of the mTOR network, we still do not know which of the mTOR-regulated targets contribute to the clinical response. This prevents identifying genetic alterations that can have predictive value regarding the sensitivity or resistance to mTOR inhibitors in spite of encouraging clinical results in unselected patients with HNSCC.

While conducting an in-depth PI3K–mTOR–pathway specific analysis of genetic alterations in HNSCC, we found that a high percentage of lesions exhibit loss of at least one copy of *EIF4E-BP1*. This gene encodes a translational repressor, 4E-BP1, which blocks the translation of a subset of growth promoting genes (reviewed in refs. 15 and 16). Specifically, cap-dependent translation initiation is activated by binding of mRNA to the eukaryotic initiation factor complex, eIF4F, which is comprised of several subunit proteins: eIF4A, eIF4E, and eIF4G (15, 16). eIF4E physically binds to the m^7G cap structure at the 5′ end of the mRNA, and eIF4G functions as a scaffold by interacting with eIF4E, eIF4A and eIF3 (15, 16). eIF4E–eIF4G association is essential for cap-dependent translation initiation (15, 16). 4E-BP1 (eIF4E-binding protein 1) and its related 4E-BP2 and 4E-BP3 proteins, displace eIF4G by binding to eIF4E, thereby preventing translation initiation (15, 16). This interaction of 4E-BPs with eIF4E is disrupted upon phosphorylation by mTOR in its mTORC1 complex (17, 18). This finding, and the emerging role of protein translation control in cancer growth (15, 16, 19), prompted us to explore whether 4E-BP1 contributes to HNSCC progression and its therapeutic response to mTOR inhibition. We provide evidence that *EIF4E-BP1* acts as tumor-suppressive gene in HNSCC, and that the therapeutic response to mTOR blockade is dependent, at least in part, on the ability to reactivate 4E-BP1 translation–repressive function. We also provide evidence that 4E-BP1 protein levels and status of phosphorylation may represent mechanistic biomarkers predicting sensitivity to mTORi in HNSCC.

Materials and Methods

Cell lines and tissue culture

Human head and neck cancer cell lines Cal33 and HN12 were developed as part of the NIDCR Oral and Pharyngeal Cancer Branch cell collection and have been described previously (4, 20). All cell lines underwent DNA authentication by multiplex short tandem repeat profiling (Genetica DNA Laboratories, Inc.) prior to the described experiments to ensure consistency in cell identity. No presence of *Mycoplasma* were found according to Mycoplasma Detection Kit-QuickTest from Biomake. All cells were cultured in DMEM containing 10% FBS supplemented with antibiotic/antimycotic solution at 37°C in the presence of 5% CO_2.

DNA constructs and lentivirus

Cal33 and HN12 cells stably expressing the reverse tetracycline-controlled transactivator fused to VP16 (rtTA) were generated by infection with pLESIP rtTA lentivirus. A phosphorylation-defective mutant of 4E-BP1 (T37A, T46A, S65A, and T70A, 4E-BP1 M) was engineered using appropriate oligonucleotides and the QuikChange II method, and cloned into a tetracycline-inducible lentiviral vector tagged with GFP (pLTI-GFP-4E-BP1 mut; refs. 21, 22). An empty GFP vector was used as a control. After lentivirus infection, 4E-BP1 mut (fused to GFP) was expressed in cells by adding doxycycline to the medium, and GFP^+ cells were sorted by FACS.

CRISPR/CAS9

Lenti-CRISPR-v2 plasmid was purchased from Addgene. A single guide RNA (sgRNA) to facilitate genome editing was designed according to Zhang Lab protocol (23). The sgRNAs of *4E-BP1* are as follows: forward, 5′CACCGCACCACCCGGCGAGTGGCG3′; reverse, 5′AAACCGCCACTCGCCGGG-TGGTGC3′.

Immunoblot analysis

Cells were lysed in lysis buffer supplemented with protease phosphatase inhibitors, and Western blot assays were performed as described previously (24). See Supplementary Materials for additional details.

7-methyl GTP pull-down and immunoprecipitation assay

Cell lysates were incubated with γ-Aminophenyl-m7GTP (C10-spacer)-Agarose (catalog no. AC-155L) from Jena Bioscience or incubated with Protein A Agarose (catalog no. 16–125) from EMD Millipore), conjugated with elF4G antibody. Beads were washed three times with lysis buffer. Proteins were released with SDS–PAGE loading buffer and analyzed by Western blot analysis using the antibodies listed above.

In vivo mouse experiments and analysis

All the animal studies using HNSCC tumor xenografts and oral carcinogenesis studies in wild-type and *4e-bp1*/2 double knockout (KO) mice were approved by the Institutional Animal Care and Use Committee of University of California, San Diego with protocol ASP # S15195. See Supplementary Materials for additional details.

IHC

IHC analysis of pS6, 4E-BP1, p4E-BP1, cleaved caspase-3, and Ki67 were performed following our previously reported procedures (24). Staining for 4E-BP1 and p4E-BP1 in human HNSCC was performed on tissue arrays (US Biomax OR601a). See Supplementary Materials for additional details.

RNA isolation from RNA-binding proteins, polysome analysis, and qPCR

To isolate RNA from ribonucleoprotein elF4G, we used protocols as described previously (25). To analyze polysome profiling, we used protocols as described previously (26, 27). For qPCR, see Supplementary Materials for additional details and Supplementary Table S1 for the list of oligonucleotides.

Published OnlineFirst March 20, 2019; DOI: 10.1158/0008-5472.CAN-18-1220

TCGA analysis

Data regarding the copy number of *4E-BP1*, analysis of disease-free or overall survival of an HNSCC cohort, and analysis DNA methylation–mediated gene silencing were all extracted from the cBio Portal for Cancer Genomics (http://www.cbioportal.org/public-portal/). See Supplementary Materials for additional details.

Statistical analysis

Data analyses, variation estimation, and validation of test assumptions were performed with GraphPad Prism version 7 for Windows (GraphPad Software). See Supplementary Materials for additional details. The asterisks of figures denote statistical significance (nonsignificant or ns, $P > 0.05$; *, $P < 0.05$; **, $P < 0.01$; and ***, $P < 0.001$). All the data are reported as mean ± SEM.

Results

Loss of 4E-BP1 expression in HNSCC: poor patient prognosis and enhanced carcinogenesis in *4e-bp1/2* KO mice

While analyzing genetic alterations in the PIK3CA–mTOR pathway in HNSCC, we observed that although the *4E-BP1* gene (*EIF4E-BP1*) is rarely mutated, at least one gene copy is lost in over 35% of patients with HNSCC (34.9% heterozygous and 1.4% homozygous, respectively; Supplementary Fig. S1A). To begin exploring the importance of *4E-BP1* loss in the progression of HNSCC, we initially analyzed the correlation between genomic alterations and disease-free (Fig. 1A;, $n = 181$, $P = 0.0004$) and overall (Supplementary Fig. S1B; $n = 511$, $P = 0.0061$) survival of patients with HNSCC from TCGA. In both analyses, *4E-BP1* gene loss was a strong predictor of poor prognosis.

At the protein level, we evaluated the expression of 4E-BP1 and phospho-4E-BP1 (p4E-BP1, 4E-BP1 phosphorylated in Thr37/46) in HNSCC tissue microarray (TMA, $n = 49$) sections by IHC (Fig. 1B). In the TMA, we observed 4E-BP1 expression loss in 16% ($n = 8$) of the HNSCC cases, with 67% ($n = 33$) of the cases displaying moderate expression. As controls, no immune staining for 4E-BP1 was observed in *eif4e-bp1/2* KO mice (Fig. 1C), and in HNSCC cells in which *4E-BP1* was genome edited (see below), but rescued by reexpression of the corresponding gene (Supplementary Fig. S1C). Analysis of the HNSCC TCGA cohort showed that DNA copy number of *4E-BP1* was significantly correlated with both mRNA ($n = 511$, $P < 0.0001$) and protein ($n = 351$, $P < 0.0001$) expression of 4E-BP1 (Supplementary Fig. S1D). Although homozygous deletion of *4E-BP1* can occur in 1.4% of HNSCC cases (above), reduced expression could also result from loss of one gene copy and gene or promoter methylation of the remaining allele. Indeed, we observed a strong correlation between gene expression and DNA methylation in the gene body of *4E-BP1* (Fig. 1D; Supplementary Fig. S2A; $n = 566$, $P < 0.001$). We also examined the status of phosphorylation of 4E-BP1, p4E-BP1 (Thr37/46) by IHC, and found that 71% ($n = 35$) of the cases in the HNSCC TMA sections were positive ($n = 49$), whereas all cases that lack detectable 4E-BP1 protein expression were also negative for p4E-BP1, thus serving also as an internal control. As additional controls, p4E-BP1 immunodetection was lost in CRISPR/Cas9–targeted *4E-BP1* HNSCC cells and rescued by reexpression of wild-type 4E-BP1 but not of a mutant that cannot be phosphorylated in the corresponding residues (Supplementary Fig. S1C and see below), and its immunodetection was abolished by mTOR inhibition (see below). This suggests that in most HNSCC cases in which 4E-BP1 is expressed, this translational inhibitor is persistently phosphorylated, thus repressing its function (15, 16).

To investigate whether *4E-BP1* loss contributes to HNSCC progression, we examined the impact of *4E-BP1/2* (*eif4e-bp1/2*) gene deletion (28) on cancer development in the oral-specific 4NQO-carcinogenesis model (13). These mice lack *4e-bp1* immune reactivity (Fig. 1C). *4e-bp1/2* KO mice do not develop tumors spontaneously (28, 29), and as expected, these mice did not exhibit spontaneous HNSCC lesions. However, we found that they are highly susceptible to chemically induced (4NQO) oral carcinogenesis. These KO mice had nearly double the number of squamous carcinomas in the tongue, and these tumors were larger than those in wild-type C57Bl/6 mice (Fig. 1E and F; Supplementary Fig. S2B). Collectively, these findings and the analysis of the HNSCC oncogenome revealing that a high percentage of lesions exhibit loss of 4E-BP1 function, either by gene copy loss, gene methylation, or persistent phosphorylation, suggest that 4E-BP1 may represent a potential tumor suppressor in HNSCC.

Dephosphorylation of 4E-BP1 disrupts translation-initiating complexes and is sufficient to prevent HNSCC tumor growth

mTOR regulates ribosomal biogenesis and protein synthesis through at least two eukaryotic translation regulators, 4E-BP1 and p70S6K (p70-S6 kinase); the latter phosphorylates ribosomal protein S6 (S6) and several initiation factors, including eIF4B (17, 30). To confirm the contribution of 4E-BP1–regulated ribosomal biogenesis and protein synthesis in this process, we took advantage of a 4E-BP1 mutant protein engineered previously (15, 16), in which the residues T37, T46, S65, and T70 were all mutated to alanine (termed 4E-BP1 M; Fig. 2A). This mutant cannot be regulated by mTOR due to lack of phosphorylated residues, thus mimicking the accumulation of the hypophosphorylated form of 4E-BP1 (termed de-phospho-Thr46-4E-BP1) induced by mTOR inhibition and its consequent effect on cap-dependent translation (31). We conditionally expressed 4E-BP1 M in representative HNSCC cells, HN12 and Cal33, both of which exhibit elevated mTOR activity, as most SCC cell lines (4, 20). These cells harbor wild-type and *PIK3CA* mutant, respectively (20). Cells expressing DNA vector or rtTA (reverse tetracycline-controlled transactivator) alone served as controls. An antibody that detects 4E-BP1 only when dephosphorylated at Thr46 was used to recognize de-phospho-Thr46-4E-BP1. Expression of 4E-BP1 M increased de-phospho-Thr46-4E-BP1 levels, but did not affect mTOR signaling as it did not reduce phospho-S6 (pS6) and phospho-AKT ($pAKT^{S473}$) levels, the latter a typical target of the mTORC2 complex (Fig. 2B; ref. 32). To explore whether expression of 4E-BP1 M in HNSCC can disrupt the protein–protein interactions between eIF4E and eIF4G, both key elements of translation–initiation complex, we used m7GTP pulldown and eIF4G immunoprecipitation (IP) experiments (scheme in Supplementary Fig. S3A and S3B). This study revealed that expression of 4E-BP1 M in Cal33 and HN12 HNSCC cells did not change the expression of eIF4E and eIF4G (Fig. 2B), but disrupted their association (Fig. 2C and D; Supplementary Figs. S3C and S4A–S4D). Remarkably, inducible expression of 4E-BP1 M halted HNSCC tumor growth (Fig. 2E and F; Supplementary Fig. S4E and S4F). Of importance, this mutant did not affect S6 phosphorylation (Fig. 2G and H), suggesting that in HNSCC disruption of the 4E-BP1 signaling branch may be sufficient to cause tumor reduction, in spite of a pS6 accumulation.

Published OnlineFirst March 20, 2019; DOI: 10.1158/0008-5472.CAN-18-1220

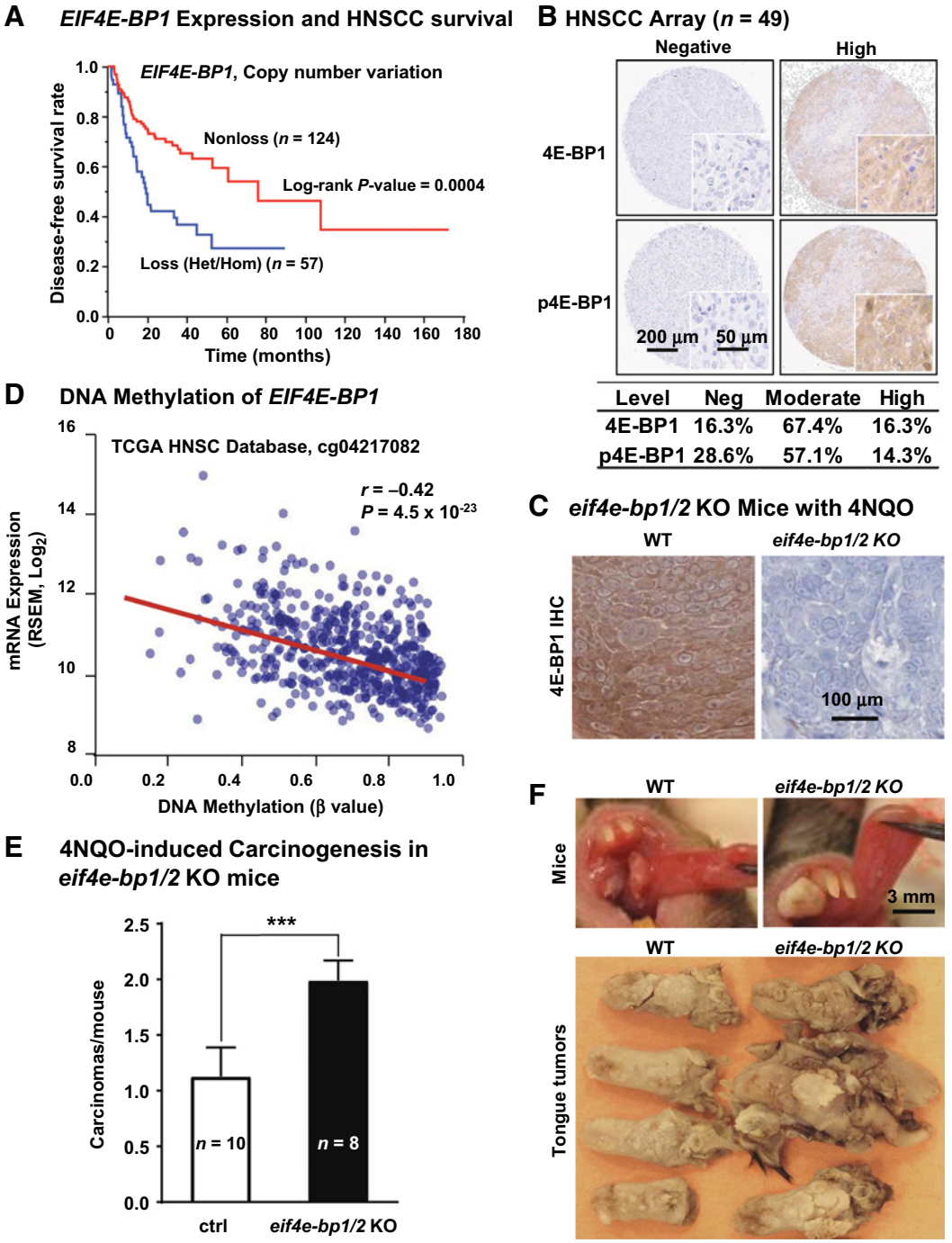

Figure 1.

EIF4E-BP1 is a candidate HNSCC tumor–suppressive gene. **A,** The TCGA database was used to determine the relationship between *EIF4E-BP1* copy number variation and disease-free survival. Data of copy number variation predicted by GISTIC algorithm were available for 181 patients with HNSCC in disease-free survival (log-rank test; $P = 0.0004$). Nonloss includes normal, copy gain, and amplification. Loss includes heterozygous deletion and homozygous deletions. **B,** Top, representative cores of HNSCC lesions stained with total 4E-BP1 (4E-BP1) and phospho-4E-BP1 (p4E-BP1, Thr37/46) using a HNSCC TMA. Bottom, the intensity of staining was scored as described previously ($n = 49$; ref. 6) and divided into negative-, moderate-, and high- expressed groups. **C,** Representative IHC analysis of 4E-BP1 in wild-type (WT) and *eif4e-bp1/2* KO mice, respectively. **D,** Significant negative correlation between DNA methylation and gene expression in the first intron of *EIF4E-BP1*, suggestive of DNA methylation–mediated gene silencing ($n = 566$, $r = -0.42$, $P = 4.56 \times 10^{-23}$). **E,** 4NQO-induced carcinogenesis in *eif4e-bp1/2* KO mice. Numbers of squamous cell carcinomas at the end of 4NQO-carcinogen treatment (mean ± SEM, $n = 10$ wild-type mice; $n = 8$ *4e-bp1/2* KO mice). **F,** Top, representative pictures of live mice tongue in wild-type and *eif4e-bp1/2* KO mice on week 26 of 4NQO treatment. Bottom, representative pictures of tongue lesions in wild-type and *eif4e-bp1/2* KO mice on week 26 (time point when mice were sacrificed) of 4NQO treatment. These tumors in *eif4e-bp1/2* KO mice were larger than those in WT C57Bl/6 mice.

Published OnlineFirst March 20, 2019; DOI: 10.1158/0008-5472.CAN-18-1220

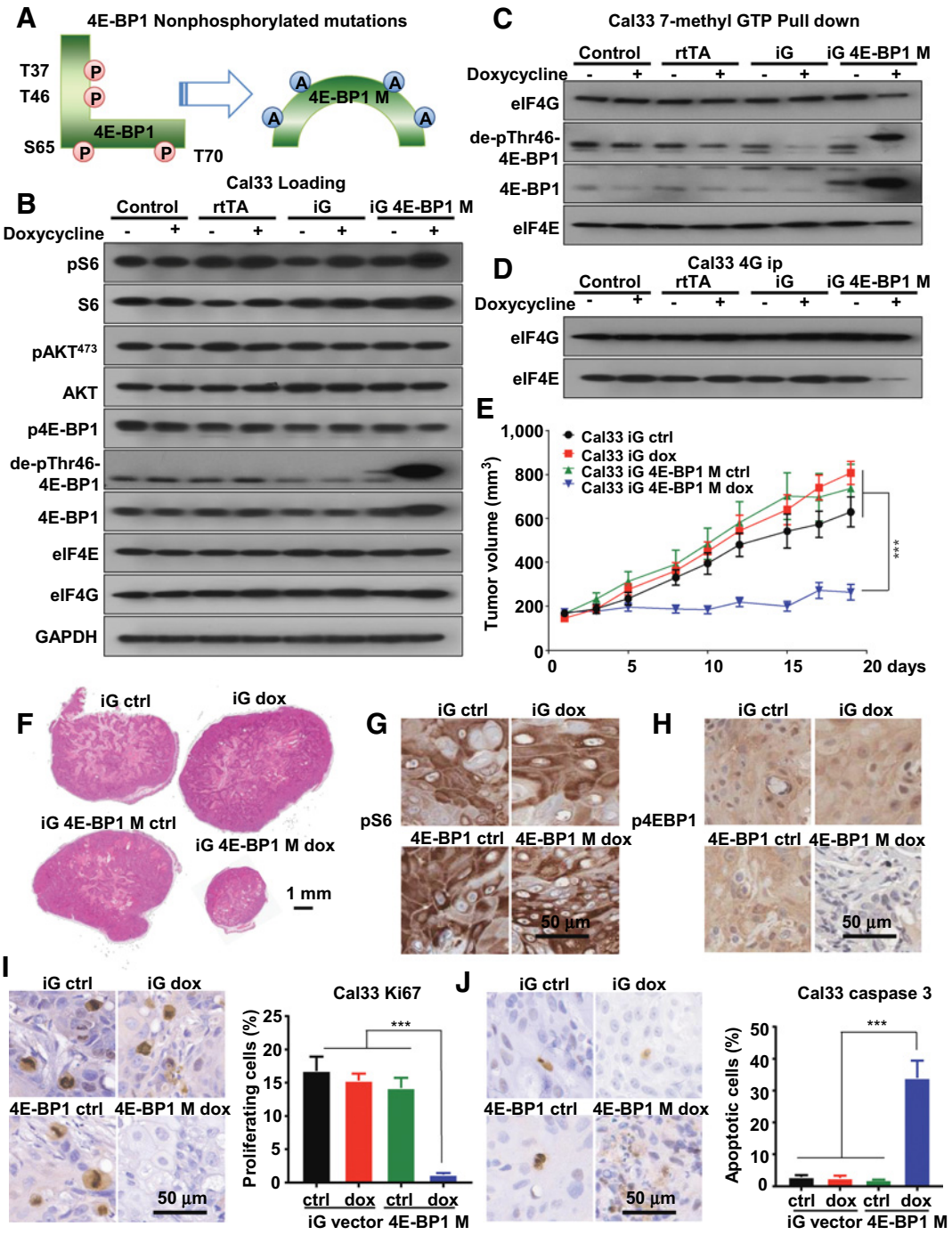

Figure 2.

Reduced growth and apoptotic effect of HNSCC cells engineered to express a mutant form of 4E-BP1 lacking mTOR phosphorylation sites. **A,** Scheme of 4E-BP1 M. The amino acids T37, T46, S65, and T70 of 4E-BP1 were mutated into alanine (A). This 4E-BP1 M remain nonphosphorylated when expressed. **B,** Western blot analysis of signaling events in HNSCC expressing 4E-BP1 M. Wild-type Cal33 cells (control), cells expressing rtTA (rtTA), cells infected with rtTA and inducible GFP fusion empty lentiviral virus (iG), or cells infected with rtTA and inducible GFP fusion 4E-BP1 M lentiviral virus (iG 4E-BP1) were turned on by doxycycline for 2 days, and lysates were analyzed as indicated. **C** and **D,** 7mGTP pull down (**C**) and eIF4G co-IP (**D**) analyzing the regulation of complex formation by 4E-BP1. Cells (same as **B**) were treated as described above and analyzed as indicated. **E,** Cal33 cells expressing empty vector (iG) or 4E-BP1 M (iG 4E-BP1 M) were transplanted into athymic nude mice, and when they reached approximately 200 mm^3, mice were fed with either regular food (ctrl) or doxycycline (dox) to turn on 4E-BP1 M expression. ***, $P < 0.001$ when comparing the 4E-BP1 M group with empty vector groups or 4E-BP1 control group (regular food) mice ($n = 10$/group). **F,** Representative histologic tissue sections from each treatment group in **E**. Scale bars, 1 mm. **G** and **H,** Representative IHC analysis of pS6 and p4E-BP1 in tumors from **E**. **I** and **J,** Representative IHC analysis (left) and quantification (right) of Ki67 and cleaved caspase-3 in tumors from **E**. Data are represented as mean ± SEM, $n = 3$ in each group.

Published OnlineFirst March 20, 2019; DOI: 10.1158/0008-5472.CAN-18-1220

Moreover, IHC for Ki67 and cleaved caspase-3 showed that, 4E-BP1 M also caused a reduction of cell proliferation and increased cell apoptosis in HNSCC tumors (Fig. 2I and J), similar to mTOR inhibition (see below).

INK128, an mTOR kinase inhibitor, displays antitumor effect in HNSCC and disrupts the translation–initiation eIF4F complex through 4E-BP1

As 4E-BP1 acts downstream of mTOR, we asked whether mTOR inhibition is sufficient to influence its tumor-suppressive effect in HNSCC. For these studies, we used rapamycin (sirolimus), a first generation of mTOR allosteric inhibitor (33), and INK128 (also known as MLN-0128 and TAK-228), which is representative of a second generation of small-molecule active-site mTOR kinase inhibitors (34, 35). As expected, both rapamycin and INK128 decreased pS6 levels. Interestingly, both drugs decreased p4E-BP1 and increased de-phospho-Thr46-4E-BP1 levels, with INK128 exerting a stronger effect. INK128 also decreased pAKT^{S473} levels, a typical target of the mTORC2 complex (32), while rapamycin did not (Fig. 3A). Although ERK was reported in some studies to inhibit 4E-BP1 function (36), in our study, inhibition of ERK with trametinib, a MEK1/2 inhibitor, had limited effect on the levels of phosphorylated 4E-BP1, as determined with use of p4E-BP1 and dephospho-Thr46-4E-BP1 antibodies. Rapamycin and LY294002, which inhibit mTORC1 and PI3K, respectively, the latter acting upstream of mTOR, served as additional controls (Supplementary Fig. S5A). Immunoblotting, m7GTP pull-down and eIF4G co-IP experiments revealed that mTOR inhibition promotes the association of 4E-BP1, and specifically its dephosphorylated form, with eIF4E, and disrupts the association

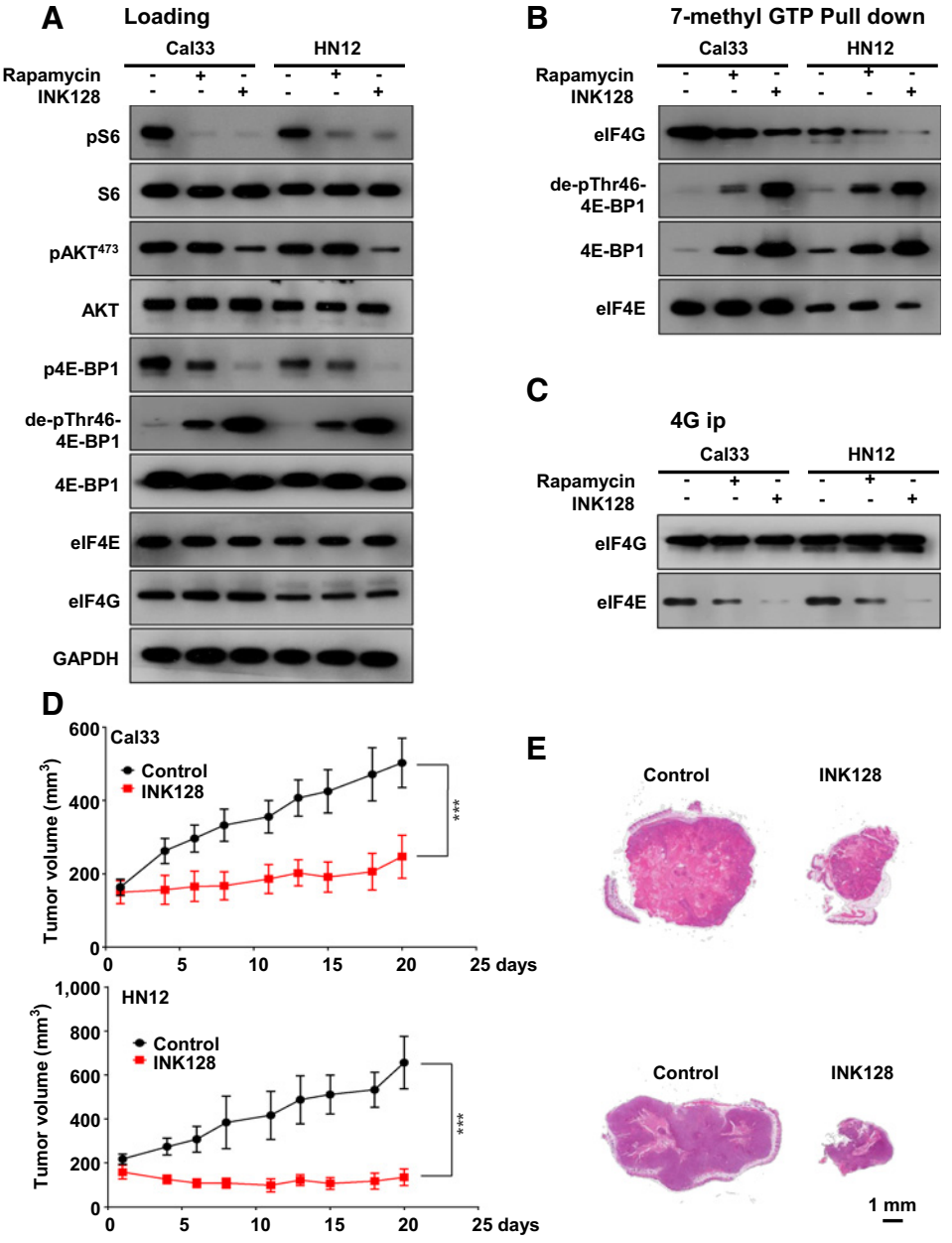

Figure 3.
Antitumor effect of mTOR kinase inhibition with INK128 and disruption of 4E-BP1 protein complexes. **A,** Western blot analysis of signaling events in HNSCC cells treated with mTOR inhibitors. Cal33 and HN12 cells were treated with rapamycin (20 nmol/L) or INK128 (20 nmol/L) for 1 hour, and lysates were analyzed as indicated. **B** and **C,** 7mGTP pull down (**B**) and eIF4G co-IP (**C**) to analyze the regulation of translation–initiation complex formation by mTOR inhibition. Cells (similar to **A**) were treated as described above and analyzed as indicated. **D,** Cal33 (top) and HN12 (bottom) were transplanted into athymic nude mice, and when they reached approximately 200 mm^3, mice were treated with vehicle diluent or INK128 for approximately 20 days, as indicated. **E,** Representative histologic sections from each treatment group in **D**. Scale bars, 1 mm. (***, $P < 0.001$ when compared with the control-treated group, $n = 10$/group).

Published OnlineFirst March 20, 2019; DOI: 10.1158/0008-5472.CAN-18-1220

between eIF4E and eIF4G (Fig. 3B and C; Supplementary Fig. S5B). Aligned with the results of 4E-BP1 dephosphorylation (above), INK128 showed higher effect than rapamycin. This provided a strong rationale for the preclinical evaluation of the efficacy of INK128 in HNSCC. Indeed, we observed that INK128 displays potent antitumor effects, achieving statistically significant differences in tumor burden as early as three days after treatment initiation (Fig. 3D and E; $n = 10$, $P < 0.001$).

CRISPR/Cas9 targeting of *4E-BP1* in HNSCC reduces the sensitivity to mTOR inhibition and reveals a role for the mTOR/4E-BP1 axis in the regulation of mRNA translation of proliferative genes

To further explore the role of 4E-BP1 in the antitumor activity of mTOR inhibition, we targeted *4E-BP1* in Cal33 and HN12 HNSCC cell lines using the CRISPR/Cas9 system. Nearly complete 4E-BP1 expression suppression was achieved (Fig. 4A). In these CRISPR/Cas9–targeted *4E-BP1* cells (*4E-BP1* CCT), mTOR inhibition remained sensitive to reduce pS6 levels. As expected, mTOR inhibition in cells lacking 4E-BP1 did not result in changes in p4E-BP1 and total 4E-BP1 levels, with slight immunoreactivity remaining likely revealing the presence of few cells retaining residual 4E-BP1, or due to cross-reactivity with 4E-BP2 (Fig. 4A; Supplementary Fig. S4A). In light of these results, disruption of the eIF4E/eIF4G complex by mTOR inhibition was almost completely reversed in *4E-BP1* CCT cells compared with parental cells (Fig. 4B and C; Supplementary Fig. S5C and S6A–S6D). We next investigated the molecular mechanism by which 4E-BP1 may mediate cancer progression in HNSCC. We isolated mRNAs associated with eIF4G, the component of the eIF4F cap–binding complex that binds mRNAs (15, 16). Initially we used a targeted approach, based on prior findings that SOX2 (37) and cyclin D1 (CCND1; ref. 38) can be regulated by eIF4E/4E-BP1–dependent translation, and observed decreased association of these well-known HNSCC proliferative (20) genes, with eIF4G (Fig. 4D and E). This prompted us to also explore whether *BMI1*, a key HNSCC cancer–proliferative and stemness gene (39), is also regulated by 4E-BP1. Indeed, *BMI1* mRNA association with eIF4G was significantly reduced by mTORi treatment, which was reflected by reduced expression levels. Of importance, in *4E-BP1* CCT cells, INK128 was less effective compared with its parental cells (Fig. 4E), supporting the conclusion that translation of these

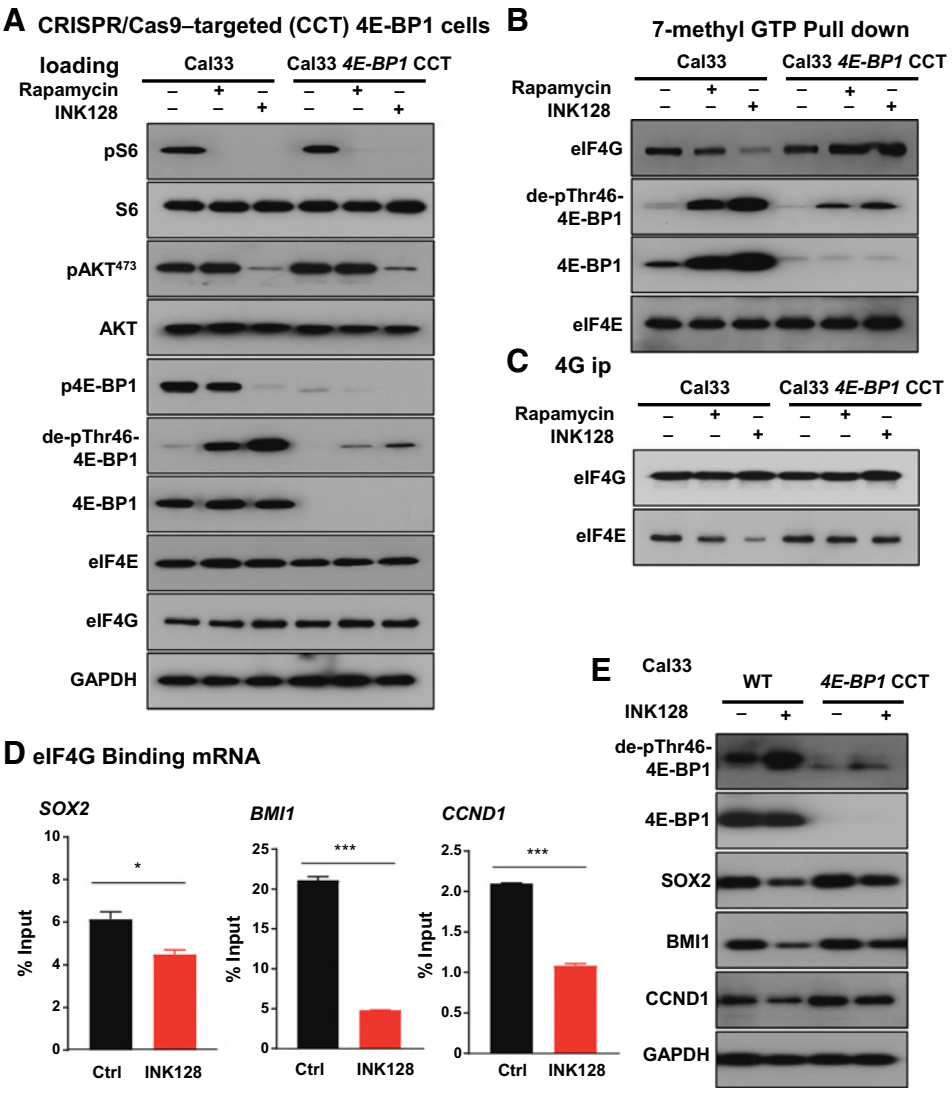

Figure 4.

CRISPR/CAS9–targeted *4E-BP1* HNSCC cells result in insensitivity to mTORi *in vitro* and reveal a role for 4E-BP1 in the regulation of the expression of proliferative molecules. **A,** CRISPR/Cas9–targeted 4E-BP1 cells *4E-BP1* CCT were achieved. Western blot analysis of signaling events in HNSCC cells treated with mTOR inhibitors. Cal33 and Cal33 *4E-BP1* CCT cells were treated with rapamycin (20 nmol/L) or INK128 (20 nmol/L) for 1 hour, and lysates were analyzed as indicated. **B** and **C,** 7mGTP pull down (**B**) and eIF4G co-IP (**C**) analyses of the regulation of translation–initiation complex formation by mTOR inhibition. Cells (similar to **A**) were treated as described above and analyzed as indicated. **D,** Cal33 cells were treated with INK128 for 2 days, the lysates were subjected to eIF4G co-IP, and associated RNAs analyzed (bound RNA). The same treated lysates were used to isolate total RNA. RNAs were followed by qPCR to assess the 4G-binding levels of regulated genes. Data are mean ± SEM % of total input (*, $P < 0.05$; ***, $P < 0.001$ when compared with the control-treated group, $n = 3$/group). **E,** Cells were treated by INK128 for 2 days; lysates were analyzed as indicated.

Published OnlineFirst March 20, 2019; DOI: 10.1158/0008-5472.CAN-18-1220

HNSCC growth–promoting genes is dependent on 4E-BP1 expression and phosphorylation status.

To further investigate the impact in translational control caused by mTOR inhibition in HNSCC, polysome-bound mRNAs were isolated by sucrose gradient fractionation after INK128 treatment of Cal33 HNSCC cells, and subjected to RNA sequencing. The complete list of genes whose polysome association was significantly altered by mTOR inhibition is shown in Supplementary Table S2. We compared this gene list with those whose mRNA translation has been previously reported to be regulated by mTORC1 in mouse embryonic fibroblasts and prostate cancer (40, 41), and developed an extended list of shared genes of interest based on their relevance to HNSCC. These included *CCNA2*, *CCNE1*, *CCNE2*, *BMI1*, *PCNA*, *EZH2*, *Eef2*, *eIF4B*, and *ODC1*, and validated them in *4E-BP1* CCT tumor samples and 4E-BP1 M–expressing cells. First, the protein expression of these selected molecules was dependent on 4E-BP1 expression and phosphorylation status in HNSCC (Fig. 5A). Moreover, their mRNA association with eIF4G was significantly reduced by INK128 treatment as well as in 4E-BP1 M cells, and the mTORi-induced reduction was rescued in *4E-BP1* CCT tumors (Fig. 5B and C), thus supporting their translational control by mTOR through 4E-BP1.

mTOR inhibition resistance *in vivo* in CRISPR/Cas9–targeted *4E-BP1* HNSCC cells

The reduced sensitivity of *4E-BP1* CCT tumors to mTOR inhibition was also recapitulated in a xenograft model. INK128 had reduced antitumor activity in *4E-BP1* CCT tumors (Fig. 6A and B). Of note, the partial response of *4E-BP1* CCT tumors to INK128 may be due to other effects of mTORC1/2, such as AKT inhibition (Fig. 4A). Consistent with our *in vitro* data (Fig. 4A), mTOR inhibition reduced pS6 in *4E-BP1* parental and *4E-BP1* CCT xenografts (Fig. 6C and D). Although p4E-BP1 was reduced in parental cells, there was no p4E-BP1 immunoreactivity in CCT cells already under basal conditions. Consistent with the reduced antitumor effect of INK128 in *4E-BP1* CCT cells, this mTORi reduced Ki67 in CCT cells less effectively than in parental cells (Fig. 6E, left). Moreover, HNSCC treated with INK128 failed to accumulate cleaved caspase-3 in *4E-BP1* CCT cells, in contrast to its proapoptotic activity in wild-type cells (Fig. 6E, right).

Discussion

The elucidation of the genomic landscape of most solid tumors, including HNSCC, has provided a unique opportunity to identify new precision therapeutic options to prevent and treat cancer. Most of the cancer driver and tumor-suppressive alterations identified to date occur in a discrete number of genes whose protein products are organized in pathways and networks. For example, in HNSCC many distinct alterations, ranging from *EGFR* and *FGFR1* mutations and overexpression, *HRAS* mutations, *PIK3CA* mutations and gene amplification, as well as few mutations and copy number variations in *AKT1*, *PTEN*, and *TSC1/TSC2* converge in the activation of the PI3K–mTOR signaling circuitry (11). This prompted the exploration of the clinical benefit of PI3Ki and mTORi in this malignancy (reviewed in ref. 11). However, we still do not know the molecular events mediating the therapeutic response of these PI3K/mTORi and their mechanisms of sensitivity and resistance, which may prevent the selection of the patients that may benefit the most from these novel anticancer agents. Here, we provide evidence that 4E-BP1, a direct mTOR substrate, acts as a HNSCC tumor suppressor, and that while 4E-BP1 dephosphorylation mediates the therapeutic response to mTORi, its gene copy loss or reduced expression renders HNSCC lesions resistant to mTOR inhibition.

Indeed, we observed that one-third of HNSCC lesions lose at least one allele of *4E-BP1*, exhibiting lower progression-free and overall survival, and that *eif4e-bp1/2* double KO mice are highly susceptible to chemically induced oral carcinogenesis. We also engineered a mutant 4E-BP1 that cannot be phosphorylated by mTOR resembling de-phospho-Thr46-4E-BP1, and generated HNSCC cells expressing this mutant in a tetracycline-inducible fashion. Expression of 4E-BP1 M was sufficient to disrupt the function of the translation–initiation complex, and resulted in tumor regression in HNSCC xenograft models. Certainly, overexpression of this mutant in the context of a wild-type 4E-BP1 may have additional effects to those caused by dephosporylation of endogenous 4E-BP1, a possibility that warrants further investigation. In this regard, as a complementary approach we observed that mTORi could not affect the translation–initiation complex in *4E-BP1* CCT HNSCC cells, and that this limited the tumor-suppressive activity of mTORi. Taken together, our findings suggest that endogenous 4E-BP1 may exert tumor-suppressive activity by restraining the expression of oncogenic translational programs in HNSCC, and that cancer progression requires bypassing the growth inhibitory properties of 4E-BP1 by gene loss and methylation, or via persistent phosphorylation by mTOR. In the latter case, which involves nearly 70% of all HNSCC cases, the latent tumor-suppressive activity of 4E-BP1 can in turn be reactivated by mTOR inhibition, thus contributing to the antitumor activity of mTORi in this cancer type.

Our findings support the idea that in HNSCC, mTORi causes 4E-BP1 dephosphorylation and consequently suppresses cancer by inhibiting translation initiation. Indeed, both the mTORC1 inhibitor rapamycin and mTORC1/2 inhibitor INK128 induced the accumulation of de-phospho-Thr46-4E-BP1. Interestingly, the same dose of INK128 showed relatively higher activity in promoting 4E-BP1 dephosphorylation and disruption of eIF4E–eIF4G association, suggesting a stronger inhibition of translation initiation. The reason for this difference might be that rapamycin and its analogues (rapalogs), which represent the first generation of mTOR inhibitors, block primarily mTOR in its complex 1 (mTORC1) indirectly by binding to FKBP12; whereas INK128, which represents a second generation of mTOR inhibitors, blocks both mTORC1 and mTORC2 by inhibiting the mTOR kinase directly (34, 35), hence displaying a stronger activity (reviewed in ref. 32). Specifically, a catalytic cleft exists within FKBP12-rapamycin–binding domain of mTOR, enabling limited access to 4E-BP1 as a substrate, whereas ATP-competitive inhibitors, such as INK128, can bind deeper inside the catalytic cleft abolishing the ability to phosphorylate 4E-BP1 (42, 43).

Inhibition of translation initiation by directly targeting the eIF4E–eIF4G association represents an attractive therapeutic option. 4EGI-1, a small-molecular inhibitor that was developed to displace eIF4G from eIF4E has displayed antitumor effects (44). However, the affinity of 4EGI-1 for the eIF4G/eIF4E complex is lower than 4E-BP1 for eIF4E (45), indicating that this approach may require further optimization to achieve its full potential. Certainly, mTOR inhibition may represent a readily available, effective, and clinically relevant choice to disrupt the eIF4G/eIF4E

Published OnlineFirst March 20, 2019; DOI: 10.1158/0008-5472.CAN-18-1220

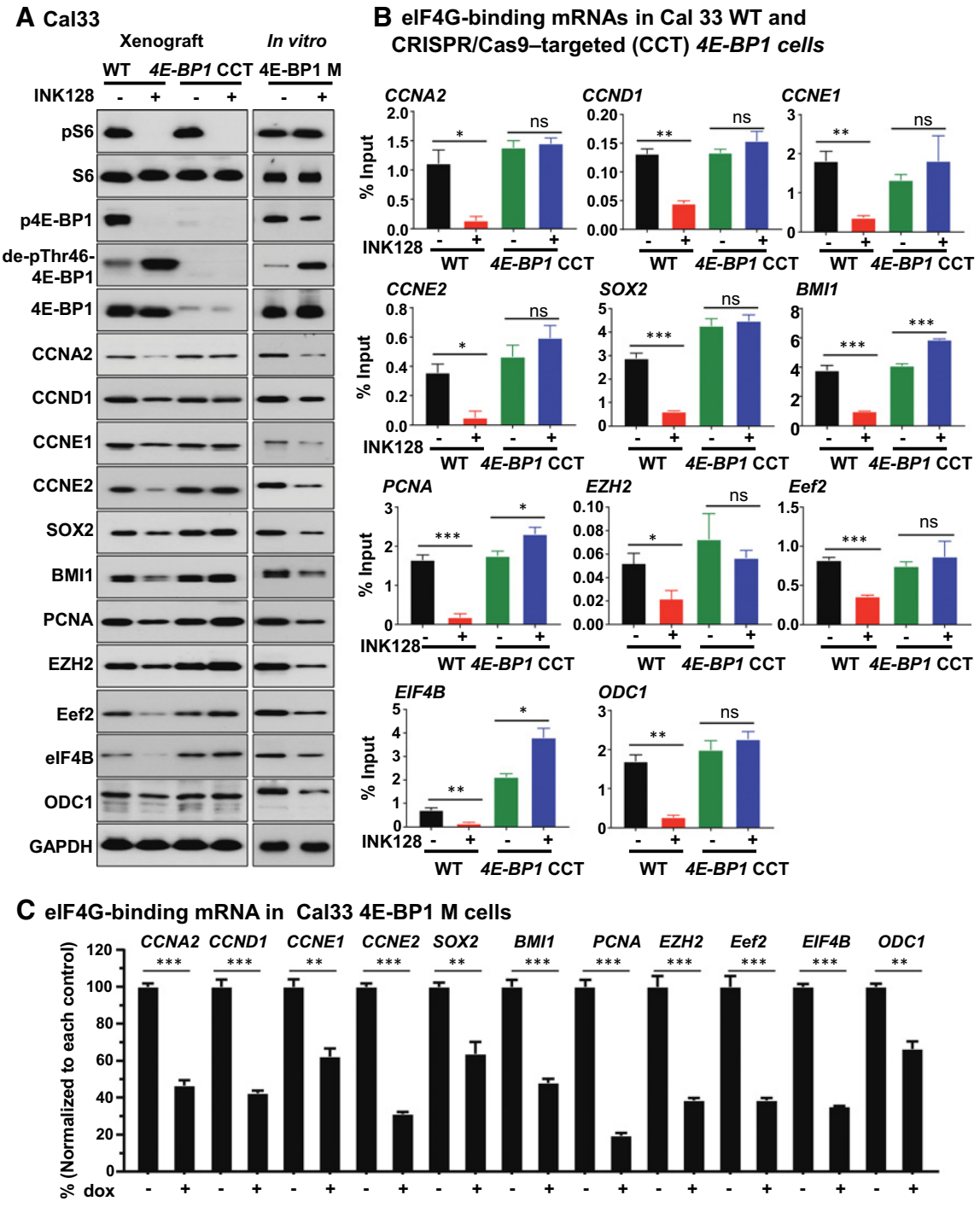

Figure 5.

Representative 4E-BP1–regulated molecules. **A,** Western blot analysis of signaling and 4E-BP1–regulated molecules *in vitro* and *in vivo* in *4E-BP1* control and *4E-BP1* CCT HNSCC xenografts (left), and HNSCC cells expressing the 4E-BP1 M (right). Left, cells were transplanted into athymic nude mice, and when they reached approximately 200 mm^3, mice were treated with vehicle diluent or INK128 for 5 days, as indicated. Right, cells infected with rtTA and inducible GFP fusion 4E-BP1 M lentiviral virus (iG 4E-BP1 M) were turned on by doxycycline for 5 days. Lysates were analyzed as indicated. **B,** The lysates of 4E-BP1 wild-type (WT) and 4E-BP1 CCT HNSCC xenografts (same as **A**) were subjected to eIF4G co-IP and associated RNAs analyzed (bound RNA). The same treated lysates were used to isolate total RNA. RNAs were followed by qPCR to assess the eIF4G-binding levels of regulated genes. **C,** The lysates of 4E-BP1 M (same as **A**) were subjected to eIF4G co-IP and associated RNAs analyzed (bound RNA). The same treated lysates were used to isolate total RNA. RNAs were followed by qPCR to assess the eIF4G-binding levels of regulated genes. For each gene, data were normalized to its control group. dox, doxycycline. Data are mean ± SEM % of total input (ns, $P > 0.05$; *, $P < 0.05$; **, $P < 0.01$; ***, $P < 0.001$ when compared with the control-treated group, $n = 3$/group).

Published OnlineFirst March 20, 2019; DOI: 10.1158/0008-5472.CAN-18-1220

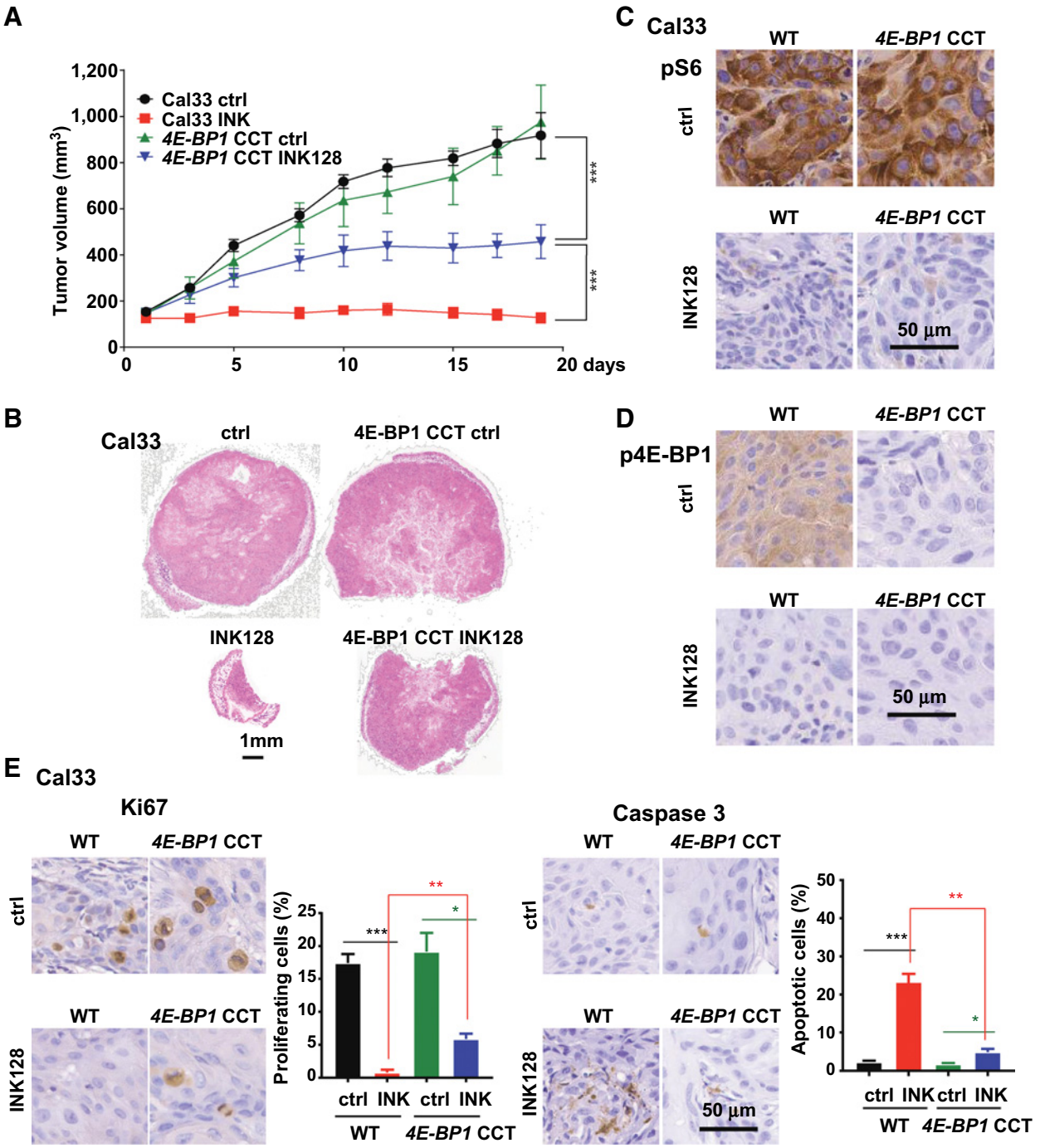

Figure 6.

Reduced sensitivity to mTOR inhibition in *4E-BP1* CCT HNSCC cells *in vivo*. **A,** Cal33 control and *4E-BP1* CCT cells were transplanted into athymic nude mice and treated with INK128. Data are the mean ± SEM of the tumor volume; ***, $P < 0.001$ when compared with the control-treated group, $n = 10$/group. **B,** Representative histologic sections from each treatment group in **A**. Scale bars, 1 mm. WT, wild type. **C** and **D,** Representative IHC analysis of pS6 (**C**) and p4E-BP1 (**D**) in tumors from **A**. **E,** Representative IHC analysis and quantification of Ki67 (left) and cleaved caspase-3 (right) to determine the percentage of apoptotic cells in tumors from A. *, $P < 0.05$; **, $P < 0.01$; ***, $P < 0.001$.

complex by unleashing the latent 4E-BP1 tumor–suppressive function in cancers expressing it. Regarding the latter, *4E-BP1* CCT cells showed reduced sensitivity *in vitro* and *in vivo* to mTORi, suggesting that 4E-BP1 expression is required for the effectiveness of mTORi. In this case, the assessment of 4E-BP1 expression and status of phosphorylation may help select patients most likely to respond to mTORi. HNSCCs in which 4E-BP1 protein is lost may not respond fully to these agents, and they may instead be suitable

Published OnlineFirst March 20, 2019; DOI: 10.1158/0008-5472.CAN-18-1220

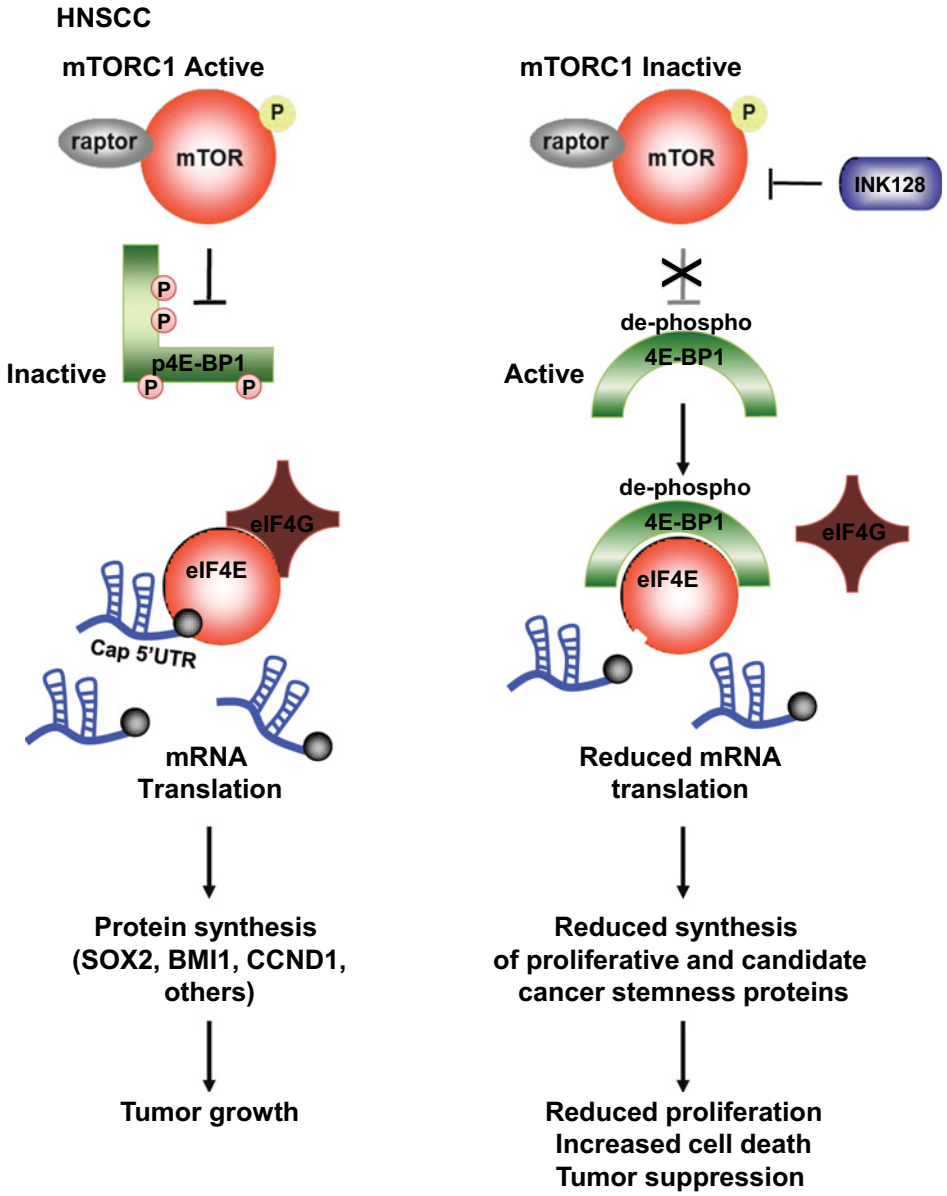

Figure 7.
Schematic representation of the mechanism by which mTOR inhibition acts in HNSCC through 4E-BP1. See Discussion for details.

candidates for future clinically relevant direct eIF4G/eIF4E complex inhibitors.

Accumulation of de-phospho-Thr46-4E-BP1, either engineered (4E-BP1 M) or when induced by INK128 administration, reduced cell proliferation and caused apoptosis in HNSCC xenografts, aligned with a proposed role for 4E-BP1 in the control of apoptosis in breast cancer, glioma, lymphomas, and other cancers (46–48). Recent high resolution transcriptome-scale ribosome profiling studies revealed the impact of mTORi on mRNA translational efficiency (40, 41). Specifically, most direct mTOR target mRNAs possess a pyrimidine-rich translational element (PRTE) and/or a 5′ terminal oligopyrimidine track (TOP) within their 5′ untranslated regions (40, 41). These include *Eef2* and *eIF4B*, two genes harboring PRTE and TOP 5′ sequences whose mRNA translation and eiF4G association were highly repressed by mTOR blockade in HNSCC, and rescued by *4E-BP1* CCT. However, prolonged mTOR blockade can also result in reduced translation of multiple mRNAs that may not harbor these targeting sequences (40, 41). Indeed, our ribosomal profiling revealed that many mRNAs are regulated by mTOR in HNSCC, including multiple drivers of HNSCC proliferation and likely cancer cell stemness, all of which were resistant to the reduction of their association to eiF4G and protein expression in *4E-BP1* CCT cells and tumors. These findings raise the possibility that multiple molecules often associated with cancer stem cells (or cancer-initiating cells) and tumor growth may be under mTOR/4E-BP1 translational control. Together, these findings support a key role for the mTOR/4E-BP1 axis in HNSCC growth, survival, and CSC characteristics, which can be exploited therapeutically for HNSCC treatment.

Overall, deep-sequencing approaches are now making it possible to identify precision medicine strategies for cancer treatment.

Published OnlineFirst March 20, 2019; DOI: 10.1158/0008-5472.CAN-18-1220

In this regard, our findings support a tumor-suppressive role of 4E-BP1 in HNSCC, and that its expression and phosphorylation status are associated with prognosis and the clinical response of mTORi in HNSCC. In addition, these findings suggest that direct mTOR kinase blockers will be even more efficacious in the clinic than its allosteric inhibitors, such as rapalogs, as they are more potent in promoting the accumulation of de-phospho-Thr46-4E-BP1, thereby restoring its endogenous growth-suppressive and proapoptotic function. Taken together, we can conclude that mTORi may unleash 4E-BP1's tumor-suppressive activity, by dephosphorylating 4E-BP1 thus reducing the translation of growth promoting, survival, and candidate cancer stemness genes, and that in turn 4E-BP1 expression and phosphorylation may serve as a prognostic biomarker for mTORi activity in patients with HNSCC (Fig. 7).

Disclosure of Potential Conflicts of Interest

No potential conflicts of interest were disclosed.

Authors' Contributions

Conception and design: Z. Wang, Q. Chen, J.S. Gutkind
Development of methodology: Z. Wang, A.A. Molinolo, D. Martin, P. Amornphimoltham
Acquisition of data (provided animals, acquired and managed patients, provided facilities, etc.): Z. Wang, X. Feng, A.A. Molinolo, D. Martin, L. Vitale-Cross, N. Nohata, A. Wahba, X. Wu, M. Gilardi, M. Allevato, V. Wu, D.J. Steffen, P. Tofilon, N. Sonenberg, J.S. Gutkind
Analysis and interpretation of data (e.g., statistical analysis, biostatistics, computational analysis): Z. Wang, A.A. Molinolo, N. Nohata, M. Ando, A. Wahba, P. Amornphimoltham, X. Wu, J. Califano, Q. Chen, S.M. Lippman, J.S. Gutkind
Writing, review, and/or revision of the manuscript: Z. Wang, L. Vitale-Cross, P. Amornphimoltham, M. Allevato, V. Wu, D.J. Steffen, P. Tofilon, N. Sonenberg, J. Califano, Q. Chen, S.M. Lippman, J.S. Gutkind
Administrative, technical, or material support (i.e., reporting or organizing data, constructing databases): Z. Wang, Q. Chen, J.S. Gutkind
Study supervision: Z. Wang, X. Feng, Q. Chen, J.S. Gutkind
Others (approval of manuscript): S.M. Lippman

Acknowledgments

The authors thank Dr. Robert A.J. Signer, Kosuke Yamaguchi, and Yusuke Goto for insightful suggestions. This project was supported by grants from National Institute of Dental and Craniofacial Research (NIH/NIDCR, 1R01DE026644, 1R01DE026870), National Natural Science Foundation of China (81602376, 81520108009, 81621062), and 111 Project of MOE (B14038), China.

The costs of publication of this article were defrayed in part by the payment of page charges. This article must therefore be hereby marked *advertisement* in accordance with 18 U.S.C. Section 1734 solely to indicate this fact.

Received April 22, 2018; revised November 7, 2018; accepted February 1, 2019; published first March 20, 2019.

References

1. Siegel RL, Miller KD, Jemal A. Cancer statistics, 2018. CA Cancer J Clin 2018;68:7–30.
2. Leemans CR, Braakhuis BJ, Brakenhoff RH. The molecular biology of head and neck cancer. Nat Rev Cancer 2011;11:9–22.
3. Chaturvedi AK, Engels EA, Pfeiffer RM, Hernandez BY, Xiao W, Kim E, et al. Human papillomavirus and rising oropharyngeal cancer incidence in the United States. J Clin Oncol 2011;29:4294–301.
4. Amornphimoltham P, Patel V, Sodhi A, Nikitakis NG, Sauk JJ, Sausville EA, et al. Mammalian target of rapamycin, a molecular target in squamous cell carcinomas of the head and neck. Cancer Res 2005; 65:9953–61.
5. Molinolo AA, Hewitt SM, Amornphimoltham P, Keelawat S, Rangdaeng S, Meneses Garcia A, et al. Dissecting the Akt/mammalian target of rapamycin signaling network: emerging results from the head and neck cancer tissue array initiative. Clin Cancer Res 2007;13:4964–73.
6. Molinolo AA, Marsh C, El Dinali M, Gangane N, Jennison K, Hewitt S, et al. mTOR as a molecular target in HPV-associated oral and cervical squamous carcinomas. Clin Cancer Res 2012;18:2558–68.
7. Stransky N, Egloff AM, Tward AD, Kostic AD, Cibulskis K, Sivachenko A, et al. The mutational landscape of head and neck squamous cell carcinoma. Science 2011;333:1157–60.
8. Agrawal N, Frederick MJ, Pickering CR, Bettegowda C, Chang K, Li RJ, et al. Exome sequencing of head and neck squamous cell carcinoma reveals inactivating mutations in NOTCH1. Science 2011;333: 1154–7.
9. Pickering CR, Zhang J, Yoo SY, Bengtsson L, Moorthy S, Neskey DM, et al. Integrative genomic characterization of oral squamous cell carcinoma identifies frequent somatic drivers. Cancer Discov 2013;3:770–81.
10. Lui VW, Hedberg ML, Li H, Vangara BS, Pendleton K, Zeng Y, et al. Frequent mutation of the PI3K pathway in head and neck cancer defines predictive biomarkers. Cancer Discov 2013;3:761–9.
11. Iglesias-Bartolome R, Martin D, Gutkind JS. Exploiting the head and neck cancer oncogenome: widespread PI3K-mTOR pathway alterations and novel molecular targets. Cancer Discov 2013;3:722–5.
12. Sun ZJ, Zhang L, Hall B, Bian Y, Gutkind JS, Kulkarni AB. Chemopreventive and chemotherapeutic actions of mTOR inhibitor in genetically defined head and neck squamous cell carcinoma mouse model. Clin Cancer Res 2012;18:5304–13.
13. Czerninski R, Amornphimoltham P, Patel V, Molinolo AA, Gutkind JS. Targeting mammalian target of rapamycin by rapamycin prevents tumor progression in an oral-specific chemical carcinogenesis model. Cancer Prev Res 2009;2:27–36.
14. Day TA, Shirai K, O'Brien PE, Matheus MG, Godwin K, Sood AJ, et al. Inhibition of mTOR signaling and clinical activity of rapamycin in head and neck cancer in a window of opportunity trial. Clin Cancer Res 2019;25: 1156–64.
15. Sonenberg N, Hinnebusch AG. Regulation of translation initiation in eukaryotes: mechanisms and biological targets. Cell 2009;136:731–45.
16. Hinnebusch AG. The scanning mechanism of eukaryotic translation initiation. Annu Rev Biochem 2014;83:779–812.
17. Hay N, Sonenberg N. Upstream and downstream of mTOR. Genes Develop 2004;18:1926–45.
18. Dowling RJ, Topisirovic I, Alain T, Bidinosti M, Fonseca BD, Petroulakis E, et al. mTORC1-mediated cell proliferation, but not cell growth, controlled by the 4E-BPs. Science 2010;328:1172–6.
19. Silvera D, Formenti SC, Schneider RJ. Translational control in cancer. Nat Rev Cancer 2010;10:254–66.
20. Martin D, Abba MC, Molinolo AA, Vitale-Cross L, Wang Z, Zaida M, et al. The head and neck cancer cell oncogenome: a platform for the development of precision molecular therapies. Oncotarget 2014;5:8906–23.
21. She QB, Halilovic E, Ye Q, Zhen W, Shirasawa S, Sasazuki T, et al. 4E-BP1 is a key effector of the oncogenic activation of the AKT and ERK signaling pathways that integrates their function in tumors. Cancer Cell 2010;18:39–51.
22. Llanos S, Garcia-Pedrero JM, Morgado-Palacin L, Rodrigo JP, Serrano M. Stabilization of p21 by mTORC1/4E-BP1 predicts clinical outcome of head and neck cancers. Nat Commun 2016;7:10438.
23. Shalem O, Sanjana NE, Hartenian E, Shi X, Scott DA, Mikkelson T, et al. Genome-scale CRISPR-Cas9 knockout screening in human cells. Science 2014;343:84–7.
24. Wang Z, Martin D, Molinolo AA, Patel V, Iglesias-Bartolome R, Degese MS, et al. mTOR co-targeting in cetuximab resistance in head and neck cancers harboring PIK3CA and RAS mutations. J Natl Cancer Inst 2014;106. pii: dju215.
25. Keene JD, Komisarow JM, Friedersdorf MB. RIP-Chip: the isolation and identification of mRNAs, microRNAs and protein components of ribonucleoprotein complexes from cell extracts. Nat Protoc 2006;1:302–7.

26. Galban S, Fan J, Martindale JL, Cheadle C, Hoffman B, Woods MP, et al. von Hippel-Lindau protein-mediated repression of tumor necrosis factor alpha translation revealed through use of cDNA arrays. Mol Cell Biol 2003;23: 2316–28.
27. Wahba A, Rath BH, Bisht K, Camphausen K, Tofilon PJ. Polysome profiling links translational control to the radioresponse of glioblastoma stem-like cells. Cancer Res 2016;76:3078–87.
28. Le Bacquer O, Petroulakis E, Paglialunga S, Poulin F, Richard D, Cianflone K, et al. Elevated sensitivity to diet-induced obesity and insulin resistance in mice lacking 4E-BP1 and 4E-BP2. J Clin Invest 2007;117:387–96.
29. Tsukiyama-Kohara K, Poulin F, Kohara M, DeMaria CT, Cheng A, Wu Z, et al. Adipose tissue reduction in mice lacking the translational inhibitor 4E-BP1. Nat Med 2001;7:1128–32.
30. Raught B, Peiretti F, Gingras AC, Livingstone M, Shahbazian D, Mayeur GL, et al. Phosphorylation of eucaryotic translation initiation factor 4B Ser422 is modulated by S6 kinases. EMBO J 2004;23:1761–9.
31. Martin D, Nguyen Q, Molinolo A, Gutkind JS. Accumulation of dephosphorylated 4EBP after mTOR inhibition with rapamycin is sufficient to disrupt paracrine transformation by the KSHV vGPCR oncogene. Oncogene 2014;33:2405–12.
32. Laplante M, Sabatini DM. mTOR signaling in growth control and disease. Cell 2012;149:274–93.
33. Guertin DA, Sabatini DM. Defining the role of mTOR in cancer. Cancer Cell 2007;12:9–22.
34. Wander SA, Hennessy BT, Slingerland JM. Next-generation mTOR inhibitors in clinical oncology: how pathway complexity informs therapeutic strategy. J Clin Invest 2011;121:1231–41.
35. Janes MR, Vu C, Mallya S, Shieh MP, Limon JJ, Li LS, et al. Efficacy of the investigational mTOR kinase inhibitor MLN0128/INK128 in models of B-cell acute lymphoblastic leukemia. Leukemia 2013;27:586–94.
36. Rolli-Derkinderen M, Machavoine F, Baraban JM, Grolleau A, Beretta L, Dy M. ERK and p38 inhibit the expression of 4E-BP1 repressor of translation through induction of Egr-1. J Biol Chem 2003;278:18859–67.
37. Tahmasebi S, Alain T, Rajasekhar VK, Zhang JP, Prager-Khoutorsky M, Khoutorsky A, et al. Multifaceted regulation of somatic cell reprogramming by mRNA translational control. Cell Stem Cell 2014;14: 606–16.
38. Averous J, Fonseca BD, Proud CG. Regulation of cyclin D1 expression by mTORC1 signaling requires eukaryotic initiation factor 4E-binding protein 1. Oncogene 2008;27:1106–13.
39. Chen D, Wu M, Li Y, Chang I, Yuan Q, Ekimyan-Salvo M, et al. Targeting BMI1(+) Cancer stem cells overcomes chemoresistance and inhibits metastases in squamous cell carcinoma. Cell Stem Cell 2017; 20:621–34.
40. Thoreen CC, Chantranupong L, Keys HR, Wang T, Gray NS, Sabatini DM. A unifying model for mTORC1-mediated regulation of mRNA translation. Nature 2012;485:109–13.
41. Hsieh AC, Liu Y, Edlind MP, Ingolia NT, Janes MR, Sher A, et al. The translational landscape of mTOR signalling steers cancer initiation and metastasis. Nature 2012;485:55–61.
42. Yip CK, Murata K, Walz T, Sabatini DM, Kang SA. Structure of the human mTOR complex I and its implications for rapamycin inhibition. Mol Cell 2010;38:768–74.
43. Yang H, Rudge DG, Koos JD, Vaidialingam B, Yang HJ, Pavletich NP. mTOR kinase structure, mechanism and regulation. Nature 2013;497: 217–23.
44. Moerke NJ, Aktas H, Chen H, Cantel S, Reibarkh MY, Fahmy A, et al. Small-molecule inhibition of the interaction between the translation initiation factors eIF4E and eIF4G. Cell 2007;128:257–67.
45. Peter D, Igreja C, Weber R, Wohlbold L, Weiler C, Ebertsch L, et al. Molecular architecture of 4E-BP translational inhibitors bound to eIF4E. Mol Cell 2015;57:1074–87.
46. Li S, Sonenberg N, Gingras AC, Peterson M, Avdulov S, Polunovsky VA, et al. Translational control of cell fate: availability of phosphorylation sites on translational repressor 4E-BP1 governs its proapoptotic potency. Mol Cell Biol 2002;22:2853–61.
47. Bi C, Zhang X, Lu T, Zhang X, Wang X, Meng B, et al. Inhibition of 4EBP phosphorylation mediates the cytotoxic effect of mechanistic target of rapamycin kinase inhibitors in aggressive B-cell lymphomas. Haematologica 2017;102:755–64.
48. Yellen P, Saqcena M, Salloum D, Feng J, Preda A, Xu L, et al. High-dose rapamycin induces apoptosis in human cancer cells by dissociating mTOR complex 1 and suppressing phosphorylation of 4E-BP1. Cell Cycle 2011; 10:3948–56.

Cancer Research
The Journal of Cancer Research (1916–1930) | The American Journal of Cancer (1931–1940)

AACR American Association for Cancer Research

4E-BP1 Is a Tumor Suppressor Protein Reactivated by mTOR Inhibition in Head and Neck Cancer

Zhiyong Wang, Xiaodong Feng, Alfredo A. Molinolo, et al.

Cancer Res Published OnlineFirst March 20, 2019.